






Coda Wave Spatial Variation in Eastern Anatolia, Turkey

Caglar Ozer^{1,2} , Mehmet Hamit Ozyazicioglu² , Sukran Perk¹ ¹ Earthquake Research Centre, Ataturk University, 25240, Erzurum, Turkey.² Department of Civil Engineering, Engineering Faculty, Ataturk University, 25240, Erzurum Turkey.

Keywords

Coda waves, seismic attenuation, coda-Q, Eastern Anatolia.

Abstract

Eastern Anatolia is a tectonically active area, where continent-to-continent collision and accretion processes are shaping the crust and leading to high seismic characteristics. The main motivation of this research is to calculate the Coda Wave Spatial Variation in the depth and horizontal plane using 3438 events recorded by 26 seismic stations. The Coda Q features from 1 to 16 Hz are computed for various lapse times, which determine the coda waves depth distribution. The contours of Q-variation in the regional crust at different depths are obtained. The Coda-Q values range from $\sim 180 \pm 120$ at 1 Hz to $\sim 800 \pm 500$ at 16 Hz in the study area. The Q characteristics are interpreted concerning tectonics, crustal anomalies, and possible geothermal regime variations. Low Q values are observed in and around major fault-lines, zones of high tectonic activity, and geothermal spots. The results suggest that 8 Hz coda-Q distribution may be associated with the Curie point depth distribution. Low Coda-Q values specifies high attenuation features, while low-frequency exponent can define clear principal attenuation according to molten lower crust along Arabian-Anatolian plate collision zone and presence old volcanic units, such as Tendürek, Agri, Süphan, and Nemrut Mountains scattered all around the study area, as well as geothermal reservoirs.

1. Introduction

One method of quantifying seismic energy attenuation is by the analysis of coda waves. The coda wave quality factor (coda-Q or Qc) gives significant information about the tectonic activity of a region. Coda-Q (Qc) varies with depth and depends on processing parameters, like lapse time, frequency, coda window length, signal to noise ratio (SNR), besides the tectonics of the region. Therefore, Havskov et al. (2016) [1] reported that the coda-Q values can allocate some tectonic regions if identical processing parameters are utilized. The coda Q is usually associated with the tectonics of the region; thus, it is related to faulting and heterogeneity of the medium. Low Qc values have consistently been obtained in tectonically active areas [2]. Moreover, some researchers [3-7] show that Qc also reduces in the close proximity of known geothermal reservoirs. This suggests that coda-Q may well be used as an indicator of potential geothermal resources if supplemented with other evidence.

Several works have been applied to define the crustal and lithospheric features beneath Eastern Anatolia. Zor et al. (2003) [8] determined the S- wave velocity structure using the receiver function method for East Anatolia. Turkelli et al. (2003) [9] found that some of the events occur in the lower-crust during the East Anatolian Fault Zone (EAFZ), whereas, mostly upper-crust earthquakes are observed throughout the North Anatolian Fault Zone (NAFZ). Sandvol et al. (2003) [10] observed a possible anisotropy in the asthenosphere beneath Eastern part of Anatolia. Gok et al. (2003) [11] declared that Eastern Anatolia was supported with a hot and thin lithospheric mantle by using Sn attenuation tomography technique. Bektas et al. (2007) [12] examined the geothermal potential using some important geophysical methods such as aeromagnetic, heat flow, and gravity in Eastern Anatolia and conclude that Curie Point Depth (CPD) from 13 to 23 km in the region. Zor (2008) [13] obtained a three-dimensional (3-D) velocity feature and stated a partially molten asthenosphere gives rise to a negative velocity anomaly beneath Eastern Anatolia. Sertcelik (2012) [2]

claimed that higher attenuation in Karliova triple junction might be evaluated as the NAFZ being effective in the upper crust. Gokalp (2012) [14] revealed a very thin lithosphere and partially molten asthenosphere in eastern Anatolia using local earthquake tomography method. Vanacore et al. (2013) [15] calculated that the Moho depth extends up to 55 km for Eastern Anatolia region and concluded that the high V_p/V_s values (>1.85) might be related to recent volcanism. Aydin (2015) [16] showed that two different attenuation areas were distinguished from south to north as Palu-Mus and Erzincan-Erzurum. Cinar and Alkan (2015) [17] determined the crustal thickness using the receiver function method was 42 km for Eastern Anatolia. Simao et al. (2016) [18] emphasized anisotropy in the new kinematic model and showed low-velocity values beneath Lake Van and surroundings in the lithospheric mantle. Sertcelik and Guleroglu (2017) [19] presented the coda feature along the NAFZ from 20 to 40 second lapse times. They presented that the coda value for NAFZ changes with frequency from 262 to 2454 for 20 sec lapse time. Ozer et al. (2019) [20] released a new 3-D seismic velocity model and reported Conrad and Moho discontinuities to be at ~ 20 km and ~ 35 km, respectively. Some coda studies have been performed in Eastern Anatolia [1, 2, 16, 21] according to recent literature. But, variation of coda-Q with depth at different frequencies is obtained for the first time in the study area. Thus, plots of spatial variation of coda-Q at different frequencies and discussions distinguish this research from earlier studies conducted in Eastern Anatolia.

2. Geology, Tectonic, and Seismic Activity

Eastern Anatolia is dominated by young volcanic units, which are related to the Miocene-Pliocene collision. Quaternary volcanism has also been observed in the region [22]. Paleozoic-Mesozoic rocks can be seen in the Bitlis massif metamorphic belt while the Malatya region contains the metamorphic [23]. Eastern Anatolia has also several basins, such as Erzincan and Erzurum basin. Erzincan Cenozoic Basin

*Corresponding Author: caglarozero@atauni.edu.tr

Received 20 Feb 2022; Revised 02 March 2022; Accepted 02 March 2022

2687-5195 /© 2022 The Authors, Published by ACA Publishing; a trademark of ACADEMY LTD. All rights reserved.

<https://doi.org/10.36937/ben.2022.4639>

is covered by younger sedimentary deposits [24]. Erzurum pull-apart basin lies between the ophiolitic mélangé of the Erzurum-Caucasus suture zone and Miocene-Pliocene volcanic. Paleotectonic and neotectonic units constitute an important part of local geology in the Erzurum basin [25].

Eastern Anatolia is a tectonic area, where progressive convergence of Arabian-Eurasian plates takes place. The crust is thus highly fractured and some of the most active tectonic units are located in this region [26-28]. The collision between the Eurasian and Arabian plates plays a significant attribute in the tectonic evolution of the Eastern Anatolian [29]. The collision has given rise to both crustal thickening and counter-clockwise tectonic escape of Anatolian Block [26]. GPS studies define that the Arabian plate makes an N-NW motion relative to Eurasia [30]. This movement between plates has given rise to ~2 km topographic elevation and a 50 km average crustal thickness [31-32] and caused the creation of the Bitlis-Zagros Thrust Belt (BZTB). The region contains two prominent fault systems, the NAFZ and the EAFZ on which many devastating earthquakes have occurred throughout history. The NAFZ and EAFZ converge in the Karlova are the two biggest active tectonic units in Turkey. The NAFZ is a dextral strike-slip fault, while EAFZ is a sinistral strike-slip fault [37-38].

In the instrumental seismological era, December 27, 1939 Erzurum and October 23, 2011 Van earthquakes resulted in a plethora of casualties and severe damages to structures. 1939 Erzurum earthquake, the largest recorded in Turkey, occurred on the east part of NAFZ on a right-lateral strike-slip fault [33-34]. More recently, 2011 Van Earthquake [35], on the other hand, displayed a relatively short surface rupture of approximately 8 km, displaying complex kinematics comprising both thrust and strike-slip components [36]. The 2011 Van earthquake source mechanism showed that the main event had a thrust focal mechanism, while the aftershocks were of strike-slip type by teleseismic waveform data [36]. Earthquake Department of Disaster and Emergency Management Authority (AFAD) fault kinematic solutions for some of the destructive events in Eastern Anatolia show that the tectonics of the region is normal, thrust, and particularly by strike-slip fault regimes.

3. Data and Method

In this study, 26 seismic stations operated by Ataturk University Earthquake Research Center (ATA-DAM), AFAD, and Georgian Seismic Network (shared with AFAD) are used (Figure 1). Only, the ERZM station is a vertical component short period seismometer (station 15 in figure 1), while the other stations host three-component broadband seismometers.

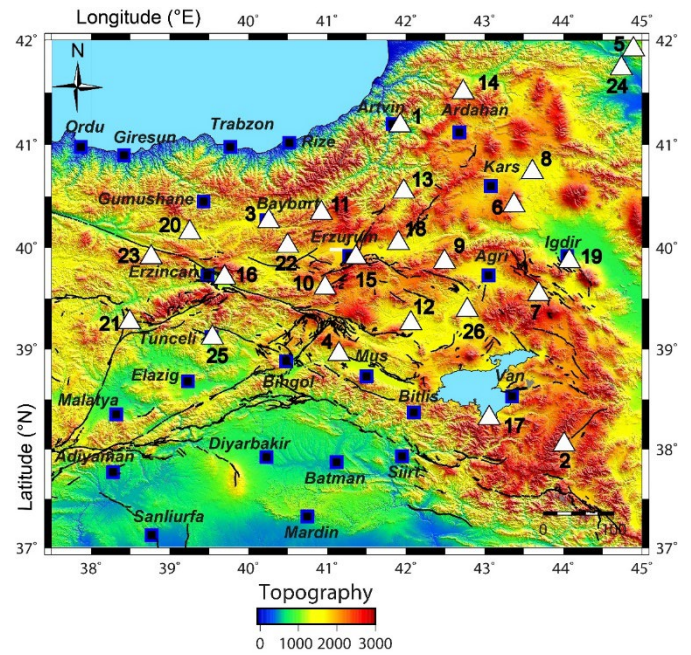


Figure 1. The seismic stations (white triangles) and the major faults [37-38] (black line) of the study area.

A total of 3438 hand-picked events ($1.0 \leq M_L \leq 6.8$) were recorded in the study area, covering Eastern Anatolia, Iraq and Syria as well as the Caucasus and the Black Sea. The distance between the epicenter and the station of these earthquakes range between 10 and 400 km (Figure 2). HYPOCENTER algorithm [39-40] in SEISAN program [41] was used to locate the earthquakes. The 3438 earthquakes are recorded between 2010 and 2015. The depths of earthquakes vary from 5 km to 50 km. Root Mean Square (RMS) values of events range from 0 to 0.5 sec.

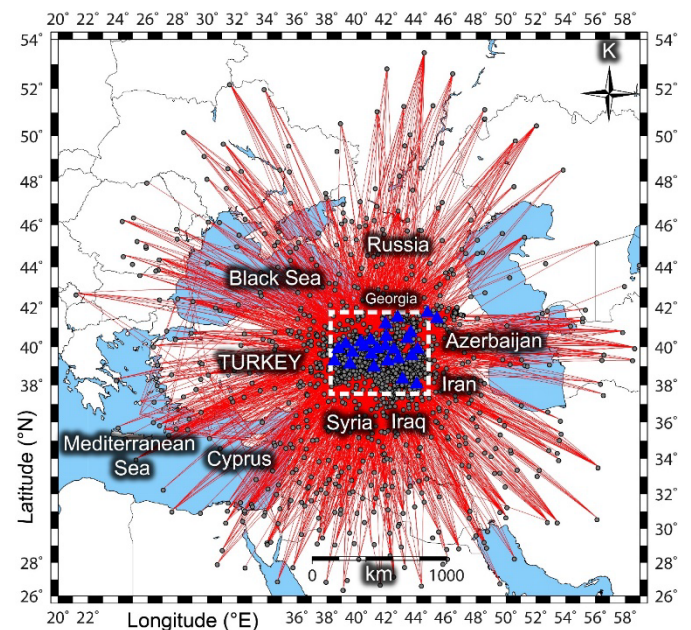


Figure 2. Ray paths of the initial catalog (red lines) (blue triangles are stations; gray circles are the earthquakes).

The coda Q spatial variation is computed by using the single backscattering method of Aki and Chouet (1975) [42] in Eastern Anatolia. In the single backscattering method, the distance between the receiver and the source is insignificant. This method defines the coda values as a superposition of secondary resources originating from scattering by heterogeneities. There is a decline in the amplitude of the coda waves with time at a special frequency. According to this method, the change of amplitude of coda waves is considered to be of the following form [42]:

$$A(f, t) = c(f) \cdot t^{-\beta} \cdot e^{-\frac{\pi f t}{Q_c}} \tag{1}$$

where, $c(f)$ is the origin function at the frequency (f), and β represents the geometrical spreading value. For body waves, β equals 1, yet it is 0.5 for Love and Rayleigh waves. $Q_c(f)$ is the coda waves quality factor [42].

The frequency of interest for Q_c values and the coda window length (30 sec) should be selected first for computing the coda-Q. The envelope is estimated by RMS averaging window. Provided that the SNR is smaller than 3, this seismogram is ignored. Then, the correlation coefficient is calculated. The minimum value of this coefficient is chosen to be 0.60 in our study. The seismograms are filtered at different frequency bands with central frequencies of 1.5, 3, 6, 12, 18, 24 Hz and with bandwidths of 1, 2, 4, 8, 12, and 16 Hz; respectively. Figure 3 represents processing an example seismogram of November 26, 2011 Van Earthquake (ML=2.9), used for coda-Q analysis in this study.

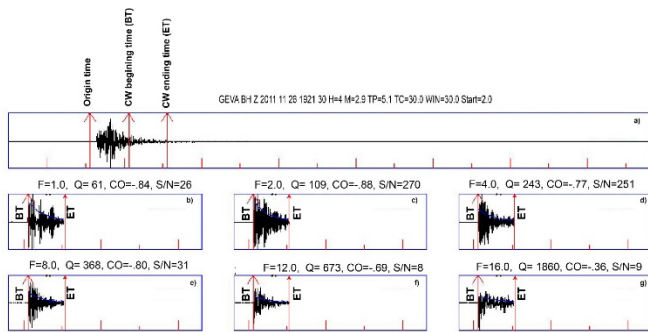


Figure 3. a) Raw Seismogram example from station GEVA and steps of coda-Q processing in SEISAN. (b) to (g) filtered coda window. Big red arrows indicate origin time, coda start and end time; respectively.

The coda-Q values are computed by codaq program in the SEISAN package [41]. Fixed lapse time is used in the computations. By the single-scattering theory, Pulli (1984) [43] claims that the volume exemplified by the coda waves is an ellipsoid, and plane projection has the following form:

$$\frac{x^2}{((Vs \cdot t)/2)^2} + \frac{y^2}{((Vs \cdot t)/2)^2 - (R/Vs)^2} = 1 \tag{2}$$

where R , shear wave velocity (V_s), t are epicentral distance, V_s and average lapse time, respectively [43], and whose foci are the source and the station. The variables x and y symbolize the surface coordinates and the x -direction for the ellipsoid is along the event-station path. It was chosen to use $V_s = 3.2$ km/sec, in compliance with the literature [20, 44]. The lapse time is the time length coming from the origin time to the coda beginning [1, 42, 43, 45]. Some researchers suggest the lapse time to be taken as $2 \cdot t_s$ (twice shear wave arrival), however, since lapse time determines the volume exemplified by the coda waves, in order not to sample different depths in one analysis, we fix the length of lapse time, as suggested by Havskov et al. (1989; 2016) [1, 46] and Havskov and Ottemöller 1999; 2010 [41, 45] (Fig. 4).

Figure 4 shows coda-Q variation at each frequency for 20, 50, 80, 100 s lapse times. The histogram is useful when analyzing coda values in different areas. There is an inverse correlation between computed Q_c values and the epicentral distance. Black plus signs indicate that for all lapse times, the number of Coda-Q decreases with epicentral distance (Figure 4).

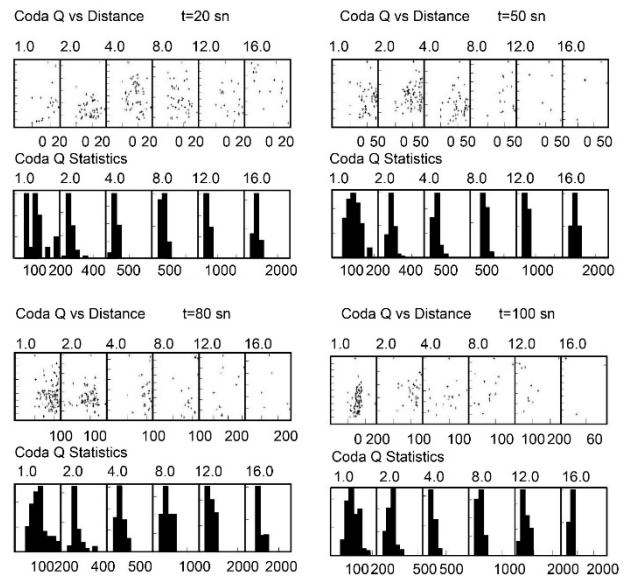


Figure 4. Coda Q results for 20, 50, 80, 100 s lapse time, respectively.

4. Results and Discussion

The Coda-Q characteristic of Eastern Anatolia is obtained by using the single-backscattering model [42] in this study. Figures 5, 6, and 7 display Coda-Q horizontal deviation for 1 Hz, 8 Hz, and 16 Hz at different depths from 8 km to 32 km. The Coda-Q values range from $\sim 180 \pm 120$ at 1 Hz to $\sim 800 \pm 500$ at 16 Hz (Figures 5, 6, and 7). This pattern proves that coda-Q increase with frequency and lapse time (i.e., with depth). Table 1 indicates the average Q_c variation expressions with the lapse time for the whole region.

It can be seen from Table 1 that Coda values at 1 Hz increases up to 90 seconds lapse time then drops, whereas the exponent α reduces with lapse time up to 90 seconds then keep almost stationary thereafter. This observation complies with the structure of the crust getting more homogenous with depth, leading to less scattering of waves and thus higher quality factor. On the other hand, since scattering is less in the lower crust (intrinsic attenuation is more pronounced), the frequency dependence of the attenuation reduces; this fact is reflected in the lower frequency exponent.

Table 1. Summary of lapse time (sec) versus derived Q_c expressions.

Lapse time (t, sec)	Coda Q \pm standard deviation	Correlation Coefficient
10	$Q_c = 77 \pm 14 f^{0.72 \pm 0.09}$	0.97
20	$Q_c = 73 \pm 7 f^{0.75 \pm 0.05}$	0.99
30	$Q_c = 88 \pm 4 f^{0.71 \pm 0.03}$	1.00
40	$Q_c = 89 \pm 6 f^{0.71 \pm 0.04}$	0.99
50	$Q_c = 93 \pm 2 f^{0.70 \pm 0.02}$	1.00
60	$Q_c = 99 \pm 1 f^{0.64 \pm 0.01}$	1.00
70	$Q_c = 94 \pm 2 f^{0.67 \pm 0.01}$	1.00
80	$Q_c = 102 \pm 3 f^{0.68 \pm 0.02}$	1.00
90	$Q_c = 104 \pm 5 f^{0.61 \pm 0.04}$	0.99
100	$Q_c = 101 \pm 4 f^{0.61 \pm 0.04}$	0.99

Q_c values at 1 Hz at 16 km depth vary from about 90 in the west of the region to around 110 in the east, near Van, Mus, and Agri provinces (Figure 5). However, at 16 Hz, Q_c values rarely exceed 700 in these regions (Figure 7). This rise in Q_c may be related to the crust thickness from the BZSZ to Pontides [8, 47, 48]. The contour maps at these depths suggest that heterogeneity decrease with increasing depth due to the absence of faulting, velocity contrasts, or decrease in fluid content. Furthermore, attenuation reduces with increasing depth.

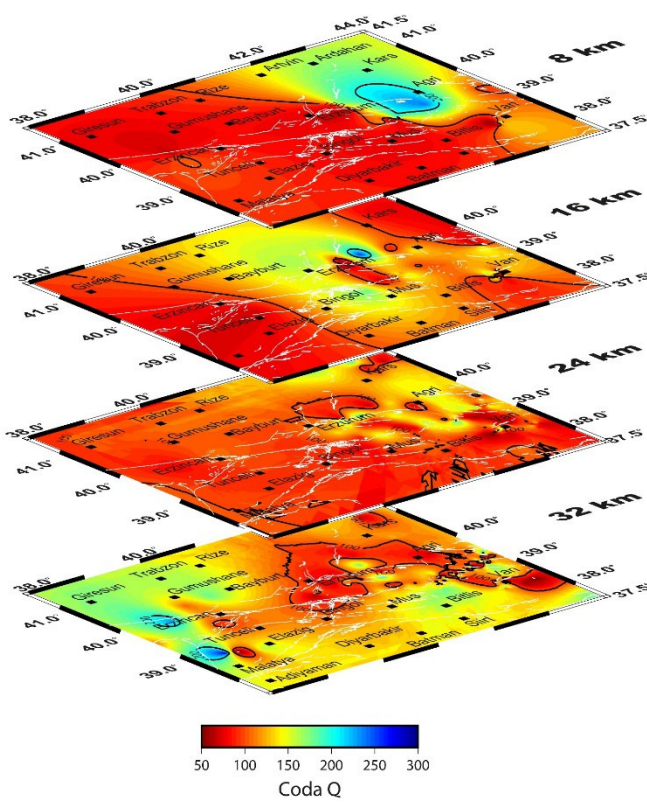


Figure 5. The spatial variation of Coda Q at 1 Hz. The white thin lines indicate main tectonic units [37, 38]. The thick black lines are the Coda Q contours.

The CPD varies according to rheological strength, geological units, mineral content, pressure and tectonic conditions [49, 50]. Knowledge of the Curie point structure of an area helps better understand the tectonic and magmatic structure of a region [51]. A Curie isotherm map of whole Turkey is given by Aydin et al. (2005) [52] helping aeromagnetic data. Furthermore, Bektas et al. (2007) [12] give the CPD map specifically for the eastern Anatolia. By comparing the Curie point maps, it is seen that there is a good relationship between the Curie point map and Qc at 8 and 16 km, especially for 8 Hz contour maps [12, 52] (Figure 6).

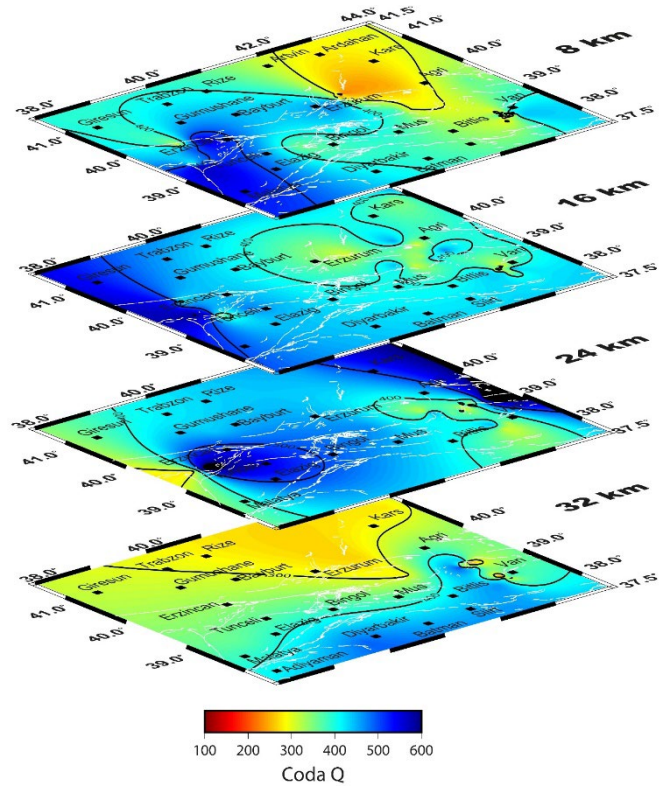


Figure 6. The spatial variation of Coda Q at 8 Hz. The white thin lines indicate main tectonic units [37, 38]. The thick black lines are the Coda Q contours.

Wave penetration has an inverse relationship with frequency, i.e., long period (low frequency) waves travel deeper into the earth [53, 54], and the wavelength is inversely proportional to the frequency. Therefore, at shallow depths more reliable results are expected of high-frequency waves. Conversely, low-frequency waves give more-accurate information about deep structures. At a depth of 16 km, Qc values in Agri and Van region exhibit an increase concerning the other regions (Figure 6). Vanacore et al. (2013) [15] claim that high Vp/Vs features may be related to recent volcanic activity. Also, the Van Lake and surrounding anomalies nearby at 1, 8, and 16 Hz are thought to be associated with young volcanic units [22, 55]. These suggest the possible existence of a correlation between the Vp/Vs ratio and spatial Coda-Q variation at 1 Hz in volcanic regions.

The Qc values also provide important details about the tectonic activity of the region. Gök et al. (2007) [56] suggest the presence of a thick and hot crust above a warm upper mantle at the Lake Van and near surroundings associated with low seismic velocity. At 16 Hz frequency, the Van region displays lower Qc values than the other regions, especially at a 16 km depth (Figure 7). For this reason, some strong anomaly must exist in this region, which may be related to strong deformation rates [18]. These lowest coda-Q zones also coincide with the epicenters of two destructive events that impact the Van province, on 23 October 2011 (Mw=7.1) and on 9 November 2011 (Mw=5.7). Consequently, it can be inferred that the low Q values, particularly at high frequencies, coincide with the zones of high tectonic activity.

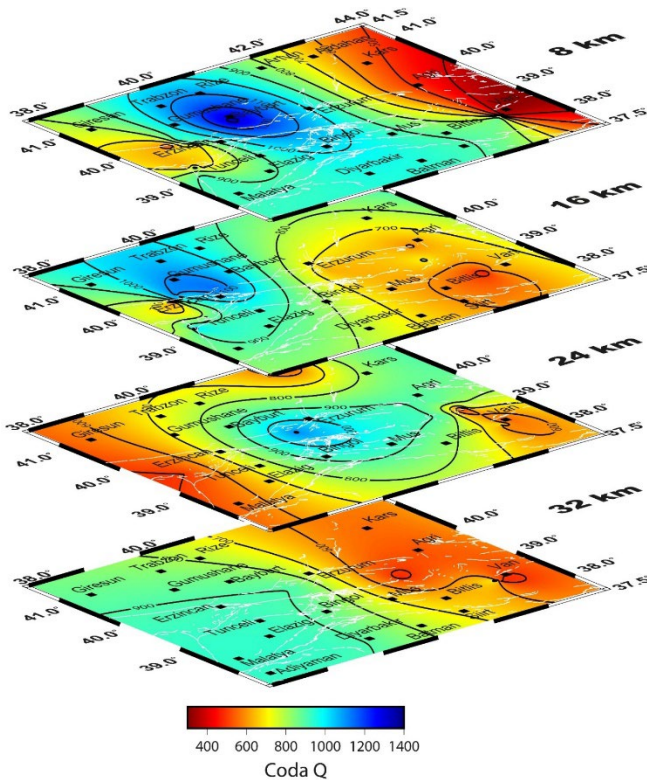


Figure 7. The spatial variation of Coda Q at 16 Hz. The white thin lines indicate main tectonic units [37, 38]. The thick black lines are the Coda Q contours.

It is well known that computed Q_c values depend strongly on processing parameters [1]. Havskov et al. (2016) [1] evaluated variation of Q_c by the processing parameters in disparate regions around the globe and introduced the idea of using optimum parameters for coda-Q estimation. Using these optimum parameters and a lapse time of 45 s, the following overall coda-Q relation is obtained for the whole region. The average values by Akinci and Eyidogan (2000) [34], Ozyazicioglu et al. (2014) [21], and Sertcelik (2012) [2] stated lower than our result, average relations by various authors are summarized in Table 2.

Table 2. Q_c expressions for Eastern Anatolia and surroundings by various researchers.

Study Area	Q_0	α
Eastern Anatolia, Turkey (this study)	91	0.70
Karliova region, Turkey [19]	189	0.86
Eastern Anatolia, Turkey [16]	97	0.93
Eastern Anatolia-Iran Border [21]	68	0.77
Eastern Anatolian Fault Zone, Turkey [2]	57.5	0.82
Zagros, Iran [57]	88	0.90
North Anatolian Fault Zone, Turkey [34]	40	0.45

5. Conclusions

Coda Wave Spatial Variation in the Eastern Anatolia at different frequencies and the variation with depth is demonstrated in this study. The Coda-Q values are evaluated by using a five-year-earthquake data set via the single backscattering method and lateral

variation of Q_c (Q contours) at various depths is obtained by varying the lapse time.

The Coda-Q varies from $\sim 180 \pm 120$ at 1 Hz to $\sim 800 \pm 500$ at 16 Hz in the study area. A regional average Q_c equation, by using the optimum parameters [1] is also obtained. Low Q_0 (91) and low-frequency exponent α (0.70) are unique to this region and distinguish Eastern Anatolia from other regions in the world when the same processing parameters are used. Low Q_0 indicates high attenuation by scattering and nonlinear (intrinsic attenuation) effects, while low-frequency exponent may point out pronounced intrinsic attenuation possibly due to molten lower crust along Arabian-Anatolian plate collision zone (Bitlis-Zagros suture) and presence of old volcanic units, like Mts. Tendürek, Agri, Süphan, and Nemrut dispersed all around the region, as well as geothermal reservoirs.

Overall, the lateral distribution of Q_0 complies with the general observations conducted in other studies, with low Q values observed in and around major fault lines and zones of high tectonic activity. Besides, this study gives the following additional results:

- There seems a high Q_0 contrast at 32 km between south and north of a line connecting Tunceli, Mus, Bingöl, Bitlis, and Van.
- Low Q_c values in the Van region are coherent with the tectonic characteristic. Remarkably, the low Q_0 zone at the south shores of the Lake Van (west of Van province) coincides with Gevaş geothermal springs.
- The results suggest that 8 Hz Coda-Q distribution may be used as a Curie point depth indicator.
- The Erzincan region has lower Q_c values at 16 Hz down to about 24 km. Similarly, at 1 Hz low Q_0 is observed in Erzincan down to 16 km. This shows the extent to which the NAFZ penetrates the crust.

Acknowledgments

The seismic waveform data is provided by the Earthquake Department of the Disaster and Emergency Management Presidency (AFAD) and Ataturk University (ATA-DAM) seismic networks. Some images are designed with GMT software [58]. The topography data sets have been collected from US Geological Survey [59] for Figure 1. The tectonic units are digitized in the Geoscience map viewer [37, 38] licensed to the General Directorate of Mineral Research and Exploration (MTA). The earthquake digital data are collected and processed in SEISAN [41] software. All computational work is conducted in the Seismological Laboratory of the Earthquake Research Center of Ataturk University, Erzurum.

Declaration of Conflict of Interests

The authors declare that there is no conflict of interest. They have no known competing financial interests or personal relationships that could have appeared to influence the work reported in this paper.

References

[1.] Havskov, J., Sørensen, M.B., Vales, D., Ozyazicioglu, M., Sanchez, G., Li, B., Coda Q in different tectonic areas, influence of processing parameters. Bulletin of the Seismological Society of America 106(2016) 965-970.

[2.] Sertcelik, F., Estimation of Coda Wave Attenuation in the East Anatolia Fault Zone, Turkey. Pure and Applied Geophysics 169(2012) 1189-1204.

- [3.] Canas, J.A., Pujades, L.G., Blanco, M.J., Soler, V., Carracedo, J.C., Coda-Q distribution in the Canary Islands. *Tectonophysics* 246(1995) 245-261.
- [4.] Mukhopadhyay, S., Sharma, J., Del-Pezzo, E., Kumar, N., Study of attenuation mechanism for Garwhal-Kumaun Himalayas from analysis of coda of local earthquakes. *Physics of the Earth and Planetary Interiors* 180(2010) 7-15.
- [5.] Naghavi, M., Rahimi, H., Moradi, A., Mukhopadhyay, S., Spatial variations of seismic attenuation in the North West of Iranian plateau from analysis of coda waves. *Tectonophysics* 708(2017) 70-80.
- [6.] Yavuz, E., Ş. Barış, Ş., Determination of coda wave attenuation characteristic of the Armutlu Peninsula and its surroundings (Middle Marmara region, Turkey). *Annals of Geophysics* 62(2019).
- [7.] Azguet, R., Bouskri, G., Timoulali, T., Harnafi, M., Yel, F., Attenuation of coda waves in the SW of High-Atlas area, Morocco. *Geodesy and Geodynamics* 10(2019) 297-306.
- [8.] Zor, E., Sandvol, E., Gurbuz, C., Turkelli, N., Seber, D., Barazangi, M., The crustal structure of the East Anatolian plateau (Turkey) from receiver functions. *Geophysical Research Letters* 30(2003) 8044.
- [9.] Turkelli, N., Sandvol, E., Zor, E., Gok, R., Bekler, T., Al-Lazki, A., Karabulut, H., Kuleli, S., Eken, T., Gurbuz, C., Bayraktutan, S., Seber, D., Barazangi, M., Seismogenic zones in eastern Anatolia. *Geophysical Research Letters* 30(2003) 8039.
- [10.] Sandvol, E., Turkelli, N., Zor, E., Gok, R., Bekler, T., Gurbuz, C., Seber, D., Barazangi, M., Shear wave splitting in a young continent-continent collision: An example from eastern Anatolia. *Geophysical Research Letters* 30(2003) 8041.
- [11.] Gok, R., Sandvol, E., Turkelli, N., Seber, D., Barazangi, M., Sn attenuation in the Anatolian and Iranian plateau and surrounding regions. *Geophysical Research Letters* 30(2003) 24.
- [12.] Bektas, O., Ravat, D., Buyuksarac, A., Bilim, F., Ates, A., Regional Geothermal Characterisation of East Anatolia from Aeromagnetic, Heat Flow and Gravity Data. *Pure and Applied Geophysics* 164(2007) 975-998.
- [13.] Zor, E., Tomographic evidence of slab detachment beneath eastern Anatolia and the Caucasus. *Geophysical Journal International* 175(2008) 1273-1282.
- [14.] Gokalp, H., Tomographic Imaging of the Seismic Structure beneath the East Anatolian Plateau, Eastern Anatolia. *Pure and Applied Geophysics* 169(2012) 1749-1776.
- [15.] Vanacore, E.A., Taymaz, T., Saygin, E., Moho structure of the Anatolian Plate from receiver function analysis. *Geophysical Journal International* 193(2013) 329-337.
- [16.] Aydin, U., Estimation of seismodynamics differences and lateral variations of coda Q in Eastern Anatolia. *Arabian Journal of Geosciences* 8(2015) 6363-6370.
- [17.] Cinar, H., Alkan, H., Crustal Structure of Eastern Anatolia from Single-Station Rayleigh Wave Group Velocities. *Eastern Anatolian Journal of Science* (2015) 57-69.
- [18.] Simao, N.M., Nalbant, S.S., Sunbul, F., Mutlu, A.K., Central and eastern Anatolian crustal deformation rate and velocity fields derived from GPS and earthquake data. *Earth and Planetary Science Letters* 433(2016) 89-98.
- [19.] Sertcelik, F., Guleroglu, M., Coda Wave Attenuation Characteristics for North Anatolian Fault Zone, Turkey. *Open Geoscience* 9(2017) 480-490.
- [20.] Ozer, C., Ozyazicioglu, M., Gok, E., Polat, O., Imaging the Crustal Structure Throughout the East Anatolian Fault Zone, Turkey, by Local Earthquake Tomography. *Pure and Applied Geophysics* 176(2019) 2235-2261.
- [21.] Ozyazicioglu, M., Sorensen, M., Havskov, J., An estimation of seismic attenuation in Eastern Anatolia by Coda-Q method. *Earthquake reality along the silk road and scientific cooperation* (2014) 11-20, ISBN: 978-975-442-695-3.
- [22.] Keskin, M., Pearce, J.A., Mitchell, J.G., Volcano-stratigraphy and geochemistry of collision-related volcanism on the Erzurum-Kars Plateau, North Eastern Anatolia. *Journal of Volcanology and Geothermal Research* 85(1998) 355-404.
- [23.] Caglayan, M.A., Onal, R.N., Sengun, M., Yurtsever, A., Structural setting of the Bitlis Massif. In: O.Tekeli, & M.C.Goncuglu (ed.), *Geology of the Taurus Belt. Proceedings of the International Symposium on the Geology of the Taurus Belt* (1984) 245-254.
- [24.] Aktar, M., Dorbath, C., Arpat, E., The seismic velocity and fault structure of the Erzincan basin, Turkey, using local earthquake tomography. *Geophysical Journal International* 156(2004), 497-505.
- [25.] Kocyigit, A., Canoglu, M.C., Neotectonic and seismicity of Erzurum pull-apart basin, East Turkey. *Russian Geology and Geophysics* 58(2017) 99-122.
- [26.] McKenzie, D.P., Active Tectonics of the Mediterranean region. *Royal Astronomical Society Geophysical Journal* 30(1972) 109-185.
- [27.] McQuarrie, N., Stock, J.M., Verdel, C., Wernicke, B.P., Cenozoic evolution of Neotethys and implications for the causes of plate motions. *Geophysical Research Letters* 30(2003) 30-33.
- [28.] Bozkurt, E., Neotectonics of Turkey—a synthesis. *Geodinamica acta* 14(2001) 3-30.
- [29.] Italiano, F., Sasmaz, A., Yuce, G., Okan, O.O., Thermal fluids along the East Anatolian Fault Zone (EAFZ): Geochemical features and relationships with the tectonic setting. *Chemical Geology* 339(2013) 103-114.
- [30.] McClusky, S., Balassanian, S., Barka, A., Demir, C., Ergintav, S., Georgiev, I., Gurkan, O., Hamburger, M., Hurst, K., Kahle, H., Kastens, K., Kekelidze, G., King, R., Kotzev, V., Lenk, O., Mahmoud, S., Mishin, A., Nadariya, M., Ouzounis, A., Paradisis, D., Peter, Y., Prilepin, M., Reilinger, R., Sanli, I., Seeger, H., Tealeb, A., Toksöz, M.N., Veis, G., Global Positioning System Constraints on Plate Kinematics and Dynamics in the Eastern Mediterranean and Caucasus. *Journal of Geophysical Research* 105(2000) 5695-5719.
- [31.] Sengor, A.M.C., Kidd, W.S.F., The post-collisional tectonics of the Turkish-Iranian Plateau and a comparison with Tibet. *Tectonophysics* 55(1979) 361-376.
- [32.] Dewey, J.F., Hempton, M.R., Kidd, W.S.F., Saroglu, F., Sengor, A.M.C., Shortening of continental lithosphere: The neotectonics of eastern Anatolia—a young collision zone, in *Collision Tectonics* In M.P. Coward and A.C. Ries (Ed.), *Geological Society Special Publications* (1986) 3-36.
- [33.] Akinci, A., Eyidogan, H., Frequency dependent attenuation of s and coda waves in Erzincan region (Turkey). *Physics of the Earth and Planetary Interiors* 97(1996) 109-119.
- [34.] Akinci, A., Eyidogan H., Scattering and anelastic attenuation of seismic energy in the vicinity of north Anatolian fault zone, eastern Turkey. *Physics of the Earth and Planetary Interiors* 122(2000) 229-239.
- [35.] Dogan, B., Karakas, A., Geometry of co-seismic surface ruptures and tectonic meaning of the 23 October 2011 Mw 7.1 Van earthquake (East Anatolian Region, Turkey). *Journal of Structural Geology* 46(2013) 99-114.
- [36.] Irmak, T.S., Dogan, B., Karakas, A., Source mechanism of the 23 October, 2011, Van (Turkey) earthquake (Mw = 7.1) and aftershocks with its tectonic implications. *Earth Planets Space* 64(2012) 991-1003.
- [37.] Emre, O., Duman, T.Y., Ozalp, S., Elmaci, H., Olgun, S., Saroglu, F., 1/1.125.000 Olcekli Turkiye Diri Fay Haritasi. *Maden Tetkik ve*

Arama Genel Mudurlugu Ozel Yayinlar Serisi (2013) <http://www.mta.gov.tr/v3.0/>. Accessed 19 June 2020.

[38.] Emre, O., Duman, T.Y., Ozalp, S., Saroglu, F., Olgun, S., Elmaci, H., Can, T., Active fault database of Turkey. *Bulletin of Earthquake Engineering* 16(2018) 3229-3275.

[39.] Lienert, B.R., Berg, E., Frazer, L.N., HYPOCENTER: an earthquake location method using centered, scaled, and adaptively damped least squares. *Bulletin of the Seismological Society of America* 76(1986) 771-783.

[40.] Lienert, B.R., Havskov, J., A computer program for locating earthquakes both locally and globally. *Seismological Research Letters* 66(1995) 26-36.

[41.] Havskov, J., Ottemoller, L., SeisAn Earthquake analysis software. *Seismological Research Letters* 70(1999) 532-534.

[42.] Aki, K., Chouet, B., Origin of coda waves: Source, attenuation and scattering effects. *Journal of Geophysical Research* 80(1975) 3322-3342.

[43.] Pulli, J.J., Attenuation of Coda waves in New England. *Bulletin of the Seismological Society of America* 74(1984) 1149-1166.

[44.] Ozer, C., Ozyazicioglu, M., The Local Earthquake Tomography of Erzurum (Turkey) Geothermal Area. *Earth Sciences Research Journal* 23(2019) 209-223.

[45.] Havskov, J., Ottemöller, L., Routine Data Processing in Earthquake Seismology. The Netherlands: Springer (2010).

[46.] Havskov, J., Malone, S., McClurg, D., Crosson, R., Coda Q for the state of Washington. *Bulletin of the Seismological Society of America* 79(1989) 1024-1038.

[47.] Tezel, T., Shibutani, T., Kaypak, B., Crustal thickness of Turkey determined by receiver function. *Journal of Asian Earth Sciences* 75(2013) 36-45.

[48.] Akin, U., Ulugergerli, E., Kutlu, S., The Assessment of Geothermal Potential of Turkey by Means of Heat Flow Estimation. *Bulletin of the Mineral Research and Exploration* 149(2014) 201-210.

[49.] Pamuk, E., Investigating edge detection, Curie point depth, and heat flow using EMAG2 magnetic and EGM08 gravity data in the northern part of Eastern Anatolia, Turkey. *Turkish Journal of Earth Sciences* 28(2019) 805-821.

[50.] Quintero, W., Campos-Enríquez, O., Hernández, O., Curie point depth, thermal gradient, and heat flow in the Colombian Caribbean (northwestern South America). *Geothermal Energy* 7(2019) 1-20.

[51.] Vargas, C.A., Pulido, J.E., Hobbs, E.W., Thermal structure of the Panama Basin by analysis of seismic attenuation. *Tectonophysics* 730(2018) 81-99.

[52.] Aydin, I., Karat, H.I., Kocak, A., Curie-point depth map of Turkey. *Geophysical Journal International* 162(2005) 633-640.

[53.] Lay, T., Wallace, T.C., Determination of Earth Structure (Chapter 7), *Modern Global Seismology*. *International Geophysics* 58(1995) 236-309.

[54.] Webb, S.C., Broadband seismology and noise under the ocean. *Reviews of Geophysics* 36 (1998) 105-142.

[55.] Akinci, A., Antonioli, A., Observations and stochastic modeling of strong ground motions for the 2011 October 23 Mw 7.1 Van, Turkey, earthquake. *Geophysical Journal International* 192(2013), 1217-1239.

[56.] Gok, R., Pasyanos, E.M., Zor, E., Lithospheric structure of the continent-continent collision zone: eastern Anatolia. *Geophysical Journal International* 169(2007) 1079-1088.

[57.] Rahimi, H., Hamzehloo, H., Lapse time and frequency-dependent attenuation of coda waves in the Zagros continental

collision zone in Southwestern Iran. *Journal of Geophysics and Engineering* 5(2008) 173-185.

[58.] Wessel, P., Smith, W.H.F., Scharroo, R., Luis, J.F., Wobbe, F., Generic Mapping Tools: Improved version released. *EOS Transactions American Geophysical Union* 94(2013) 409-410.

[59.] U.S. Geological Survey, 1996, GTOPO30. Online Links: <http://edc.usgs.gov/products/elevation/gtopo30/gtopo30.html>.

How to Cite This Article

Özer, Ç., Özyazıcıoğlu, M.H., and Perk, S., Coda Wave Spatial Variation in Eastern Anatolia, Turkey, *Brilliant Engineering*, 2(2022), 4639. <https://doi.org/10.36937/ben.2022.4639>